3967

ANALYTICAL AND NUMERICAL ASSESMENT OF FATIGUE PROPERTIES IN ROLLING BEARINGS

Paweł Romanowicz[1(*)], Bogdan Szybiński[1]
[1]Institute of Machine Design, Cracow University of Technology, Kraków, Poland
[(*)]*Email:* promek@mech.pk.edu.pl

ABSTRACT

The aim of the work is to create an algorithm of fatigue life prediction for typical rolling bearings. The proposed approach makes use of various, well established hypothesis for multiaxial fatigue applied in engineering calculations. In the first part of the work the theoretical solutions for different contact problems are compared with the numerical ones. The respective numerical results are obtained with the use of finite element modelling (ANSYS software). Then, an algorithm for fatigue life prediction is demonstrated. The results of the proposed analysis are compared with those given in rolling bearings catalogue.

Keywords: contact problem, rolling bearing, fatigue, finite element method.

INTRODUCTION

Experimental fatigue tests of rolling bearings are expensive and time-consuming. For typical load, the fatigue life of rolling bearing can be predicted using well-known relationship based on experimental tests proposed by Palmgren & Lundberg (Lundberg, 1947; Lundberg 1952): $L=(C/P)^k$, where L is the fatigue life, C is the basic load rating, P is the applied external load and k is exponent of the life equation. The application of multiaxial hypotheses in estimation of rolling bearings life time can be an alternative to the above given traditional formulae. These criteria (Papuga, 2011; Papadopoulos, 1997) require only the distributions of stresses in investigated parts of the bearing and material parameters, which can be obtained in common fatigue tests performed for the fully reversed bending and the fully reversed torsion. Subsurface stress distribution in the most dangerous points in rolling bearings can be calculated using finite element modeling (Romanowicz, 2012; Szybiński 2012). In case of ball (rolling in a non-conforming groove) or roller bearings theoretical solutions proposed for elliptical (Sackfield, 1983) or line contact (Radzimovsky, 1953) can be used alternatively, which can help to eliminate time consuming numerical calculations.

FATIGUE PROBLEMS OF ROLLING BEARINGS

Due to the cyclic contact the non-proportional high subsurface stresses occur in the rolling bearings. Due to this fact, the fatigue failure is the most important problem in such elements. However, the level of fatigue in rolling bearings cannot be calculated using classical theories based on fatigue diagrams. In this situation, the application of multiaxial high-cycle fatigue criteria offers certain possibilities of fatigue life prediction (Romanowicz, 2012). Such criteria, which can be based on the different approaches, reduce the complex stress state to the equivalent form, which in many cases is compared with the fatigue limit for the fully reversed torsion. Moreover, almost all criteria require only two standard fatigue tests – the fully reversed bending (f_{-1}) and the fully reversed torsion (t_{-1}). However, the largest difficulty is to select hypothesis which is reliable for investigated problem (Romanowicz, 2013). For analysis of rolling bearings the criterion given by Papadopoulos (Papadopoulos, 1997) was selected. Using this hypothesis, many rolling contact problems were investigated (railway wheels, cylindrical crane wheels) and some report can be found in the literature (Bernasconi, 2006; Romanowicz, 2013). This criterion is proposed for hard metals and gives the most conservative results from the popular group of criteria which is very often used for rolling contact fatigue analysis (Romanowicz, 2013). It is based on an average measure of resolved shear stress amplitude $\langle T_a \rangle$ and includes the maximal hydrostatic stress $\sigma_{H,\max}$ in the below formula:

$$\sqrt{\left(\langle T_a \rangle\right)^2} + \left(\frac{3t_{-1}}{f_{-1}} - \sqrt{3}\right) \cdot \sigma_{H,\max} \le t_{-1} \qquad (1)$$

More information and techniques about this criterion can be found in (Romanowicz, 2010). Other probabilistic and deterministic life prediction models for rolling bearings can be found in Ref. (Sadeghi, 2009).

ANALITYCAL SOLUTION

The general methods for determining the size of the contact area and the distribution of stresses for frictionless surfaces and perfectly elastic solids are based on the Hertz theory (Hertz, 1881). In the practical application of machine design the two following types of contact can be distinguished:

- circular or elliptical contact in which the bodies initially have one contact point before the deformation (Fig. 1a),
- line contact in which bodies have straight line contact before the deformation (Fig. 1b).

The first one appears in ball bearings, where balls are rolling in a non-conforming groove. The similar situation appears in spherical bearings, railway wheels moving along convex-headed rails and in contact of two cylinders with different diameters and perpendicular axes. The second one exists in case of contact of parts in the roller bearings, and between the gear teeth, etc.

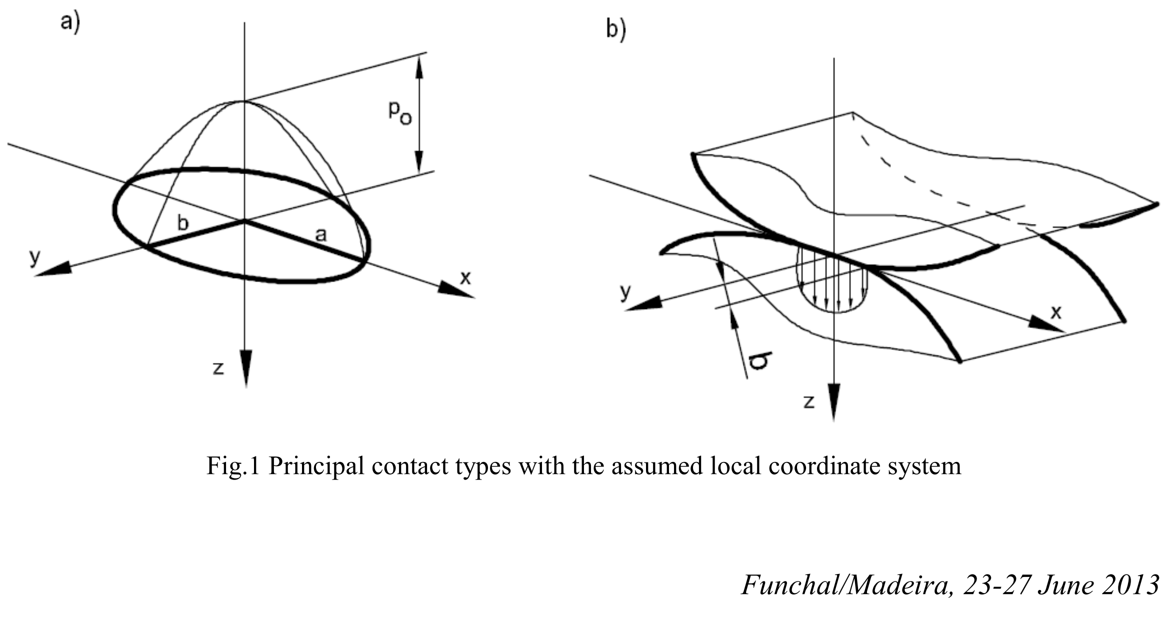

Fig.1 Principal contact types with the assumed local coordinate system

In the general case of the compression of two spherical elastic bodies, the semi axes of contact ellipse and the maximal contact pressure can be calculated from the solution given by Timoshenko and Goodier (Timoshenko, 1951). However the following assumptions must be fulfilled:

- bodies in contact are made of homogeneous and isotropic materials,
- bodies in contact have smooth surfaces with regular curvatures in the contact area,
- small elastic deformations of the bodies in the contact area,
- the loading acts in perpendicular direction to the contact surface,
- the radii of curvatures of the bodies are very large in comparison with the radius of the boundary of the contact area,
- no friction appears between surfaces (only normal stresses occur at the contact surfaces).

In order to calculate semi axes of contact ellipse the constants A and B, which depends on the contact condition, have to be found from the formulas:

$$A + B = 0{,}5\left(R_{11}^{-1} + R_{12}^{-1} + R_{21}^{-1} + R_{22}^{-1}\right), \tag{2}$$

$$B - A = 0{,}5 \cdot \sqrt{\left(R_{11}^{-1} + R_{12}^{-1}\right)^2 + \left(R_{21}^{-1} + R_{22}^{-1}\right)^2 + 2\left(R_{11}^{-1} + R_{12}^{-1}\right)\left(R_{21}^{-1} + R_{22}^{-1}\right)\cos(2\varphi)}, \tag{3}$$

where

R_{11}, R_{12} – are the minimum and the maximum principal radii of curvatures of the first body at the initial contact point, respectively,

R_{21}, R_{22} – the corresponding values of radii for the second body,

φ - the angle between the planes of principal curvatures of the two surfaces.

The magnitudes of the semi-axes of the contact area can be calculated as follows:

$$a = m \cdot \sqrt[3]{\frac{3\pi}{4}\frac{F(k_1 + k_2)}{A + B}}; \quad b = n \cdot \sqrt[3]{\frac{3\pi}{4}\frac{F(k_1 + k_2)}{A + B}}, \tag{4}$$

where

$$k_i = \frac{1 - \upsilon_i^2}{\pi \cdot E_i}; \quad i = 1, 2, \tag{5}$$

ν, *E* – Poisson's coefficient and Young modulus, respectively.

The maximal contact pressure p_o caused by the external compressive force F appears at the contact center and can by calculated as:

$$p_o = \frac{3}{2}\frac{F}{\pi \cdot a \cdot b}, \tag{6}$$

and the distribution of the contact pressure in the elliptical contact area can be expressed as:

$$p(x, y) = p_o\left(1 - x^2/a^2 - y^2/b^2\right), \quad |x| \le a, \quad |y| \le b, \tag{7}$$

where (x,y) is the local coordinate system with the origin at the contact center (initial point of contact – Fig. 1).

The values of m and n coefficients for some points (Fig. 2) can be found in the book (Timoshenko, 1951) for $\theta \in \langle 30^\circ; 90^\circ \rangle$ with the resolution 5°, or in (Cooper, 1968) for $\theta \in \langle 1^\circ; 90^\circ \rangle$ with the resolution 1°. However the continuous functions of m and n (Fig. 2), which are necessary for numerical calculations, were proposed by the authors as follows:

$$m^{-1} = -0.072576 \cdot \theta^4 + 0.306757 \cdot \theta^3 - 0.425848 \cdot \theta^2 + 0.817353 \cdot \theta + 0.018040, \tag{8}$$

$$n = -0.640562 \cdot \theta^6 + 3.471455 \cdot \theta^5 - 7.405219 \cdot \theta^4 + 7.984778 \cdot \theta^3 - 4.592703 \cdot \theta^2 + \\ + 1.771294 \cdot \theta + 0.108768, \tag{9}$$

where the auxiliary angle θ (in rad) was defined as:

$$\theta = \cos^{-1}\left(\frac{B-A}{A+B}\right). \tag{10}$$

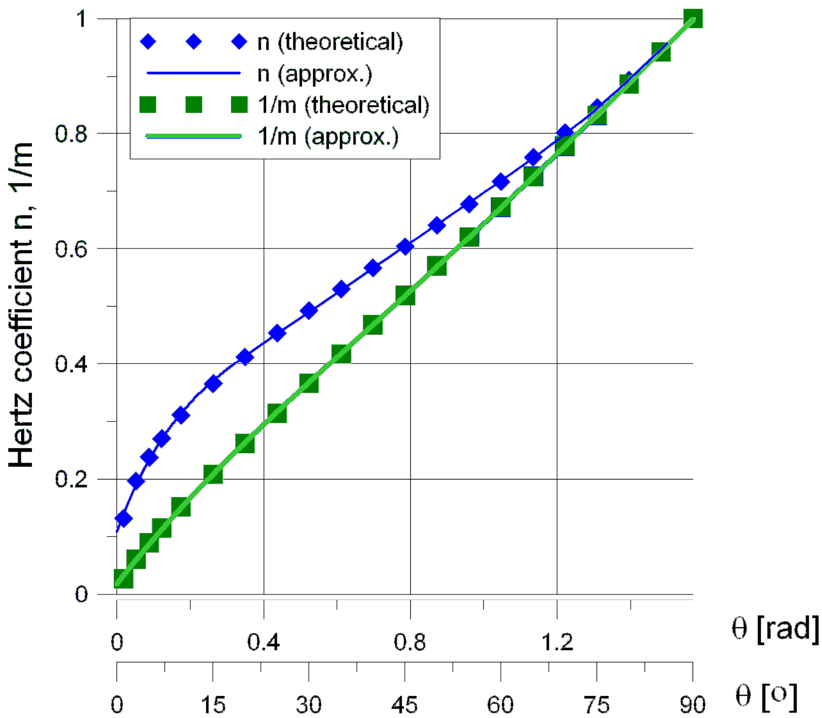

Fig. 2 The values of m and n coefficients for different contact conditions of two compressed elastic bodies.

In the simple cases of contact, the semi-axes of contact and maximum pressure can be easily calculated using the Hertz theory. The additional parameters – the relative curvature (1/R*) and E* were introduced:

$$R^* = \left(1/R_1 + 1/R_2\right)^{-1}, \tag{11}$$

$$E^* = \left(\frac{1-\nu_1{}^2}{E_1} + \frac{1-\nu_2{}^2}{E_2}\right)^{-1}, \tag{12}$$

In the case of circular contact, the axes of contact are equal and are calculated from:

$$a = b = \sqrt[3]{\frac{3P \cdot R^*}{4E^*}}. \tag{13}$$

In the case of line contact where b is the one-half of the width of the contact strip for contact of two cylinders with parallel axes (Johnson, 2004):

$$b = \sqrt{\frac{4P \cdot R^*}{\pi E^*}}, \tag{14}$$

Some useful solutions of such kind of contact were given by Hüber (Hüber, 1904) and Hamilton and Goodman (Hamilton, 1966).

In the case of elliptic contact it is more difficult to obtain explicit solution. However, if the distribution of contact pressure is known and assumption of the Hertz contact is fulfilled it is possible to calculate the stresses at any point over the contact area. First solution of this problem was proposed by Belayev in 1924 (Belayev, 1924) and Thomas and Hoersch (Thomas, 1930). They obtain distribution of subsurface stresses on the axis of symmetry by means of elliptic integrals. Another important theory including solutions determined by Fessler and Ollerton (Fessler, 1957) and Ollerton and Morey (Ollerton, 1963) was given by Sackfield and Hills (Sackfield, 1983). Using this theory the subsurface stresses over the elliptical contact area can be calculated. Some stresses $\sigma_{iz}; i = x, y, z$ can be calculated as below:

$$\begin{cases} \tau_{xz} = -p_o \cdot k \cdot x_a \cdot z_a \cdot L / \left(1 + s^2\right) \\ \tau_{yz} = -p_o \cdot k \cdot y_a \cdot z_a \cdot L / \left(k^2 + s^2\right), \\ \sigma_z = -p_o \cdot k \cdot z_a^2 \cdot L / s^2 \end{cases} \tag{15}$$

where $x_a = x/a$, $y_a = y/a$, $z_a = z/a$, $s^2 = \gamma / a^2$, $k = b/a$ and γ is the largest root of the equation:

$$1 - x^2/\left(a^2 + \gamma\right) - y^2/\left(b^2 + \gamma\right) - z^2/\gamma = 0, \tag{16}$$

and

$$L = z_a \Big/ \left[s^3 H \sqrt{\left(1 + s^2\right)\left(k^2 + s^2\right)}\right], \tag{17}$$

$$H = \left(\frac{x_a}{1 + s^2}\right)^2 + \left(\frac{y_a}{k^2 + s^2}\right)^2 + \left(\frac{z_a}{s^2}\right)^2. \tag{18}$$

The second set of the subsurface stresses can be calculated using equations:

$$\begin{cases} \sigma_{xx} = \left(\dfrac{\nu}{\pi}\right)\phi_3 - \left(\dfrac{1 - 2\nu}{2\pi}\right)\chi_{11} - \dfrac{1}{2\pi} z_a \cdot \phi_{11} \\ \sigma_{yy} = \left(\dfrac{\nu}{\pi}\right)\phi_3 - \left(\dfrac{1 - 2\nu}{2\pi}\right)\chi_{22} - \dfrac{1}{2\pi} z_a \cdot \phi_{22}, \\ \tau_{xy} = -\left(\dfrac{1 - 2\nu}{2\pi}\right)\chi_{12} - \dfrac{1}{2\pi} z_a \cdot \phi_{12} \end{cases} \tag{19}$$

where the functions ϕ_{ij}, ϕ_3, χ_{ij} were given by Sackfield and Hills (Sackfield, 1983). However, when the above formulas are in use the second set of subsurface stresses can be calculated only over the contact area.

The analytical method for determining the stress components in the case of the line contact is based on the Belayev's 3-D solution of the problem of two cylinders of infinite length pressed together (Belayev, 1924). The stresses on planes perpendicular to the coordinate axes can be calculated using following equations:

$$\begin{cases} \sigma_x = -\dfrac{2q}{\pi \cdot b} e^{-\alpha} \sin(\beta) + \dfrac{2q}{\pi \cdot b} \sin(\beta) \cdot \sinh(\alpha) \left(1 - \dfrac{\sinh(2\alpha)}{\cosh(2\alpha) - \cos(2\beta)} \right) \\ \sigma_y = -\dfrac{2q}{\pi \cdot b} \dfrac{\lambda}{\lambda + \mu} e^{-\alpha} \sin(\beta) \\ \sigma_z = -\dfrac{2q}{\pi \cdot b} e^{-\alpha} \sin(\beta) - \dfrac{2q}{\pi \cdot b} \sin(\beta) \cdot \sinh(\alpha) \left(1 - \dfrac{\sinh(2\alpha)}{\cosh(2\alpha) - \cos(2\beta)} \right) \\ \tau_{xz} = -\dfrac{2q}{\pi \cdot b} \sinh(\alpha) \sin(\beta) \dfrac{\sin(2\beta)}{\cosh(2\alpha) - \cos(2\beta)} \\ \tau_{xy} = \tau_{yz} = 0 \end{cases} \tag{20}$$

where q is loading per unit length of contact strip and λ and μ are Lame's constants, α and β are elliptic coordinates with transformation equation in respect to x-z axes (see Fig. 1b) and are given below:

$$\begin{cases} x = b \cdot \cosh(\alpha) \cdot \cos(\beta) \\ z = b \cdot \sinh(\alpha) \cdot \sin(\beta) \end{cases}. \tag{21}$$

The more detailed analysis with some useful information was given by Radzimovsky (Radzimovsky, 1953).

NUMERICAL FEM MODELS

The exemplary numerical studies were performed for two typical Hertz problems - circular and line contact. The first one, in which two rigid, ideally elastic balls are pressed to each other, was used for verification of the analytical algorithm for elliptical contact. The two balls were of the same radii and material. The high-order axisymmetric elements (ANSYS, PLANE82) and boundary conditions presented at Fig. 3 were used during these calculations. The anti-symmetric τ_{xz} shear stress distribution (the butterfly effect) with the maximal values in the P-L points was observed and is presented in the Fig. 3. Moreover, the maximal shear stress amplitude occurred on the radius of these points during the rolling contact.

In the second FEM model, which was used for verification of the algorithm for line contact, an ideally elastic cylinder was pressed to a rigid plane (Fig. 4). Due to the symmetry of investigated geometry only half of the model with plane strain assumption was computed. Moreover, the irregular meshes of high order finite elements (PLANE 82), with strong concentration of elements with regular shape in the area of stress concentration were used in both numerical models. The subsurface shear stress and the equivalent von Mises stress distributions were presented in Fig. 5, respectively. The maximal von Mises stress (Fig. 5) occurs in the Belayev point. This point is the most dangerous in the case of static contact of two bodies pressed by cyclic loadings. However, in the case of rolling contact, the cracks initiate closer to the P-L points in which the largest amplitude of shear stress caused by rolling occurs.

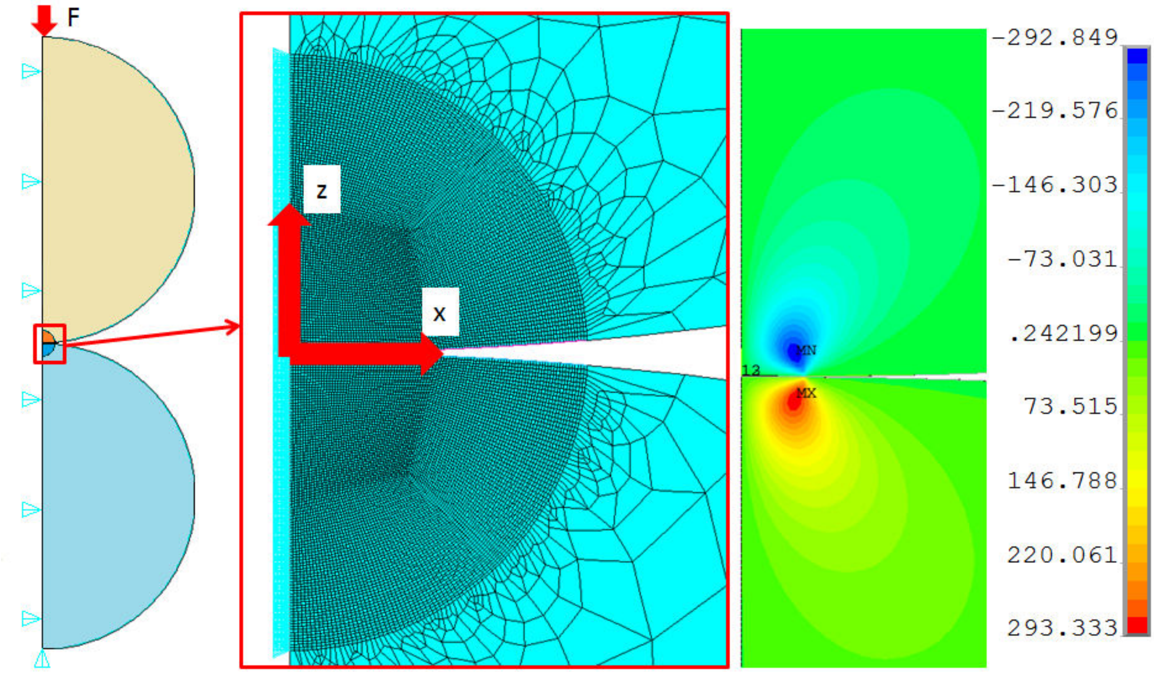

Fig. 3 Model of two compressed balls, detail of finite element mesh with local coordinate system and shear stress τ_{xz} distribution (stress in MPa)

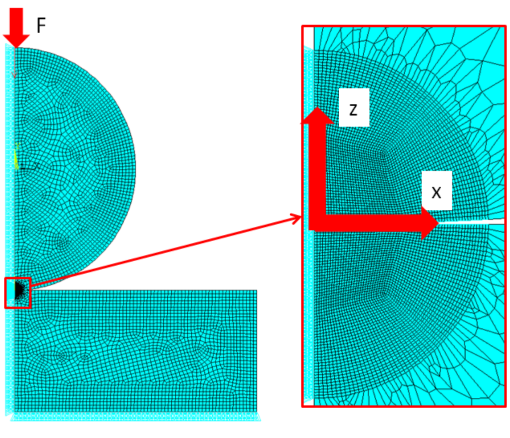

Fig.4 Model of contact of cylinder with flat plane, detail of finite element mesh with local coordinate system

For the control the subsurface stresses in four arbitrary chosen points for each model were analysed and compared with analytical solutions (for details see Fig. 1). These points were chosen in a near contact zone and one of them was the commonly used Palmgren-Lundberg (P-L) point, in which the maximum amplitude of the shear stress appears. These numerical results were compared with the respective theoretical ones. In order to estimate the solution quality the error in the form as below was proposed:

$$\Delta\sigma_i^{ERR} = \left|\frac{\sigma_i^{Theoretical} - \sigma_i^{MES}}{\sigma_i^{MES}}\right| \cdot 100\% \tag{22}$$

The summary of obtained results is given in Table 1 and as it can be seen very good agreement between theoretical and numerical results was achieved.

Table 1 Values of errors at the studied points for respective of stress tensor

Location of point [mm]			$\Delta\sigma_x^{ERR}$	$\Delta\sigma_y^{ERR}$	$\Delta\sigma_z^{ERR}$	$\Delta\tau_{xz}^{ERR}$	Remarks	model
x	y	z	[%]	[%]	[%]	[%]		
1.62	0	0.63	1.0	1.3	5E-2	0.9		Point contact (two balls pressed together) a =b = 1.85 mm p_o = 1362 MPa
0.98	0	0.48	0.4	0.6	0.2	6E-2		
0	0	1.33	1.0	1.4	0.2	- (τ_{xz} =0MPa)		
1.48	0	2.66	2.1	- ($\sigma_y \approx 0$MPa)	0.4	0.4	(P-L) point	
6.43	0	3.53	2.0	1E-4	2E-3	2E-3		Line contact (cylinder with plane) b ≈ 6 mm p_o = 1000 MPa
0.33	0	0.99	2.0	2.2E-3	9E-4	2.02		
11.36	0	10.09	0.06	0.03	2E-3	8E-4		
5.29	0	3.02	2.4	0.7	0.4	0.1	(P-L) point	

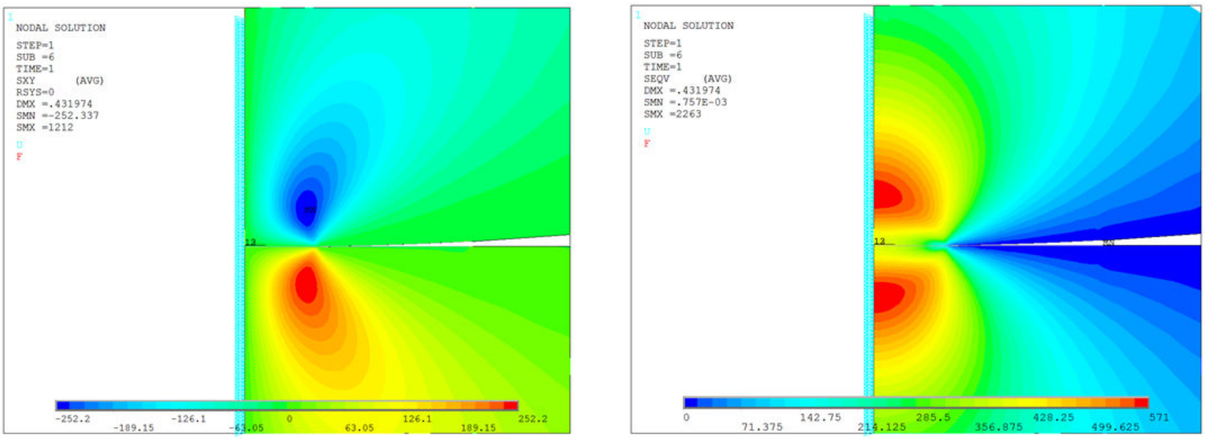

Fig. 5 The subsurface shear stress and the von Mises stress distributions in the cylinder pressed to flat plane

ANALYTICAL METHODS OF ROLLING BEARINGS CALCULATION

The presented mathematical models for elliptical contact and line contact can be applied for the investigations of the fatigue life prediction of elements working in contact conditions. In several cases it allows for the fast calculations of subsurface stresses without the application of numerical methods. The subsurface stress distribution for circular contact can be also calculated using solution given by Sackfield and Hills (Sackfield, 1983).

In the proposed models only the radii of the bodies curvatures, load per one rolling element and fatigue properties (the fully reversed bending and the fully reversed torsion) of the material are necessary. The mathematical models do not take into account friction, sliding and lubrication effects which can occur in rolling bearings. The friction between the rolling bearings is caused by different sources such as: strain hysteresis, internal friction in the lubricant, sliding and micro-sliding (caused by strains, contact geometry, gyroscopic moment, etc.), sliding between rolling elements and separator and others. The friction coefficient for rolling contact is very small and takes values from range of $\mu = 10 \cdot 10^{-4}$ for the radial ball bearing to $\mu = 40 \cdot 10^{-4}$ for the roller thrust bearing (Krzeminski-Freda, 1989).

The sliding effects between rolling element and rings can be caused by different circumferential rotational speeds of the roller and the rings contact points. It depends on the distance of these points from the axis of bearing rotation and relationship of the curvilinear pitch-surface generator of rolling elements. The oscillating micro-slip effect at the interface between two bodies, which can be attributed to difference velocities of the bodies in contact, is the source of vibration and corrosion, which results in the surface damage (fretting). More information about investigation of fretting failure of rolling bearing can be found in (Johnson, 2004). The above described phenomena do not have significant influence on the subsurface fatigue failure.

In the case of thrust rolling bearing, the force acting on one rolling element (ball or roller) can be calculated from the formulae given below

$$Q = \frac{F_a}{i \cdot Z \cdot \sin(\alpha)}, \tag{23}$$

where: F_a is the axial load of thrust bearing, i is the number of rows of rolling element, Z is the number of rolling element in one row, α is the angle between the radial and the axial components of the force.

Above equation can be used if the force is acting in the symmetry axis of bearing. However, the off-centre loading sometimes can occur. This force should be taken into account when the arm of the load in relation to the mean radius of the bearing r_m is larger than 0.6 (point contact) or 0.5238 (line contact). In such a case, the external loading is transferred by smaller number of rolling elements and maximal axial loading acting at rolling element ($Q_{max} > Q$) must be calculated (Krzeminski-Freda, 1989).

In the case of radially loaded rolling bearings by radial force F_r, the most heavily loaded ball or roller element is carrying the force:

$$Q_{\max} = \frac{F_r \cdot A_{n(\text{line, point})}}{i \cdot Z \cdot \cos(\alpha)}, \tag{24}$$

where: $A_{n(line)}$ is the coefficient of the maximal loading of the most heavily loaded roller element and $A_{n(point)}$ is the is the coefficient of the maximal loading of the most heavily loaded ball bearing element.

Certain examples of the load distribution in the function ε are presented in Fig. 6. Where ε means the coefficient of the angle of the load distribution on rolling elements. The values of the coefficient A_n for line and point contact can be estimated from the diagram presented in Fig. 7 (Krzeminski-Freda, 1989).

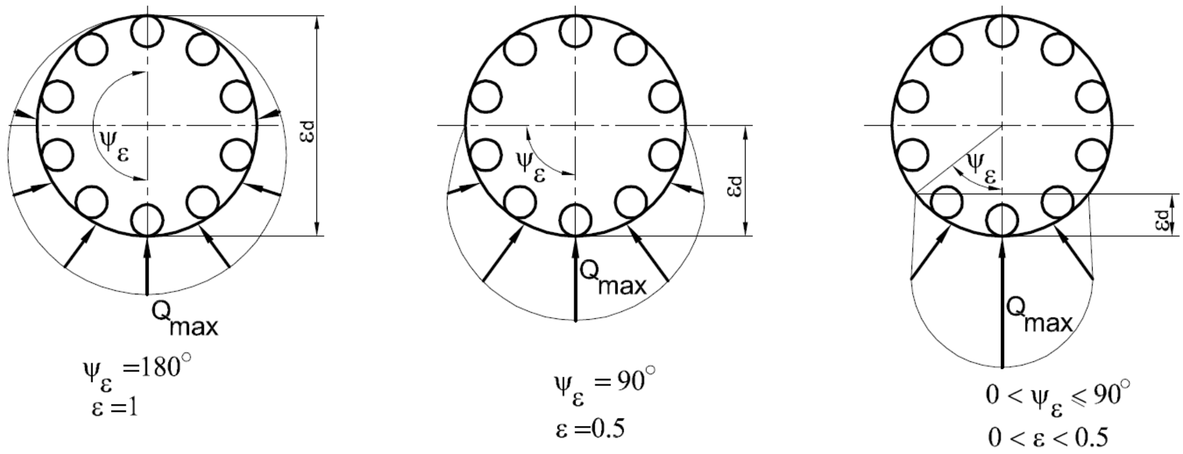

Fig. 6 Load distribution on rolling elements in radial bearing

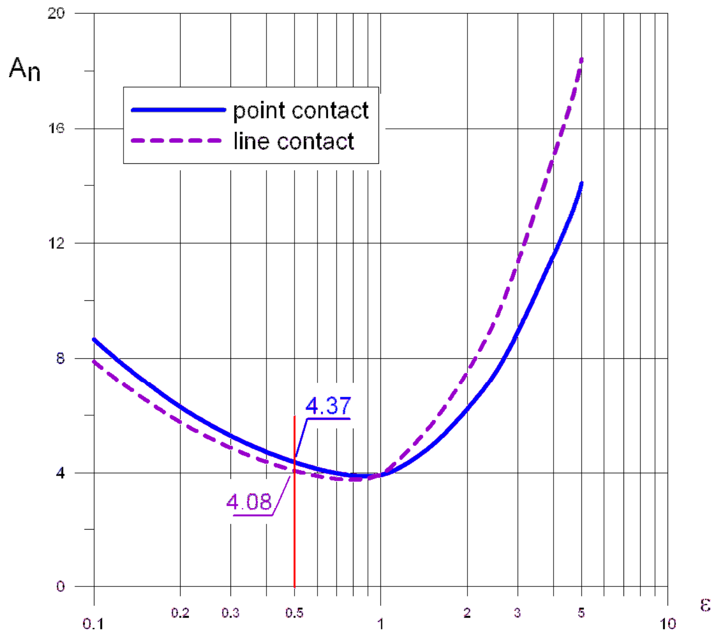

Fig. 7 The values of the coefficient A_n of the maximal loading for line and point contact

Generally, the angle Ψ_ε lies within the range of 70° ÷ 90°. In such situation, when the diameter clearance is zero the $A_{n(line)} = 4$ for roller bearings and $A_{n(point)} = 5$ for ball bearings can be assumed (Hamrock, 1983).

In order to obtain more accurate solution the total elastic deformation δ and diameter clearance P_d must be taken into account following one of the given below formulas (Hamrock, 1983):

(i) for roller bearings

$$F_r = \frac{\left[\psi_\varepsilon - \frac{P_d}{2\delta}\sin(\psi_\varepsilon)\right] Z \cdot Q_{\max}}{2\pi\left(1 - \frac{P_d}{2\delta}\right)}, \tag{25}$$

(ii) for ball bearings

$$F_r = \frac{F_{\max} \cdot Z}{J_\varepsilon}, \tag{26}$$

where

$$J_\varepsilon = \frac{\pi(1 - P_d / 2\delta)^{3/2}}{2.491\left\{\left[1 + \left(\frac{1 - P_d / 2\delta}{1.23}\right)^2\right]^{1/2} - 1\right\}}. \tag{27}$$

RESULTS AND CONCLUSIONS

The mathematical solutions for line and elliptical contact were applied in the calculations of rolling bearings. The algorithm proposed in Fig. 8 was used in the fatigue analysis of selected rolling bearings. As input data: radii of curvatures, loading per roller element, contact length, material properties (E, t_{-1}, f_{-1}, ν), start point z_{min} , end point z_{max} and no. of points of calculations were introduced.

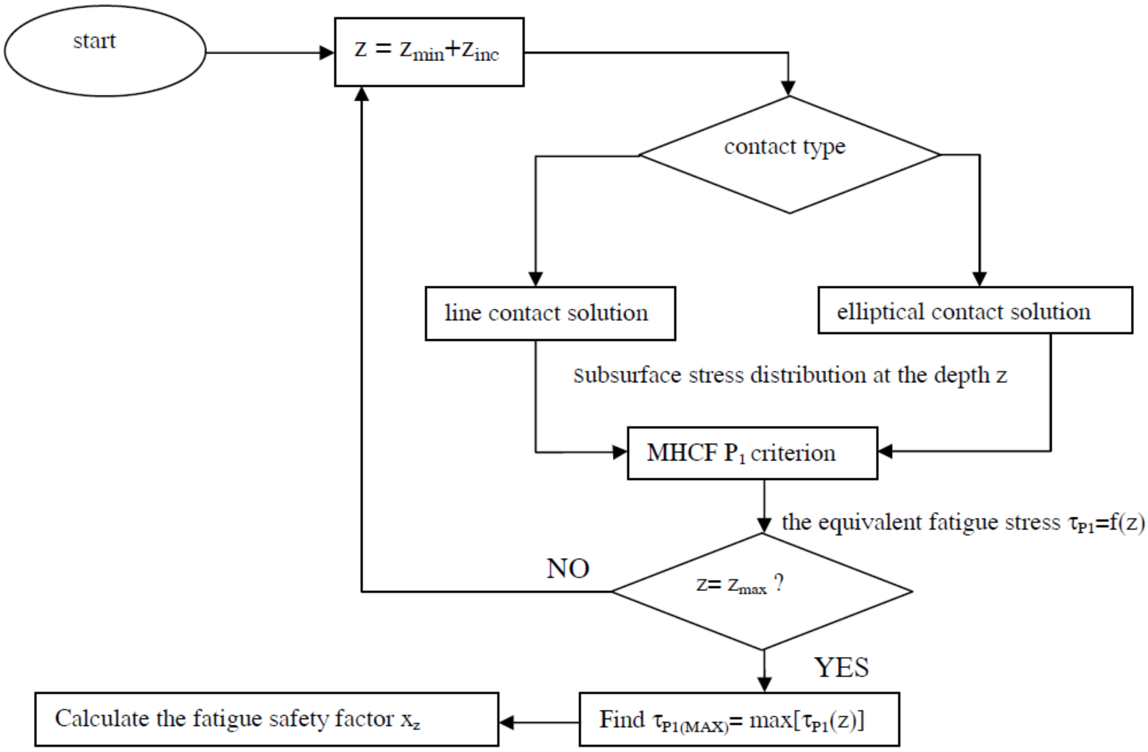

Fig. 8 The algorithm for the analytical calculation of RCF of rolling bearing

The maximal fatigue loads for the bearing made from steel X105CrMo17 were calculated. The material properties of this hard steel t_{-1}=427 MPa and f_{-1} = 712 MPa (Romanowicz, 2012) for about $10^7 \div 10^8$ cycles to failure were assumed in the performed fatigue analyses. The information about the investigated bearings are given in the table 2. The principal dimension (inside – d and outside - D diameter and bearing width – H), the basic load ratings and the fatigue load limit F_u are given by the producer (SKF). In the case of roller bearing the equivalent fatigue stress in relation to the fatigue limit - t_{-1}/τ_{P1} was calculated for the contact length set to 80% of the roller element length. Such assumption resulted from the shape of the cylindrical roller given in Ref. (Hamrock, 1983). The calculation of the safety factor for spherical roller thrust bearing was performed for the optimal radius of the roller element (Romanowicz, 2012). The more detailed information about numerical FEM analysis and high-cycle fatigue analysis of this bearing can be found in Ref. (Romanowicz, 2012).

Furthermore, the maximal fatigue loads in the sense of the multiaxial high-cycle fatigue hypothesis P_1 were calculated for the selected rolling bearings.

Table 2 Comparison of calculated fatigue stress with information given in catalogues by manufacturer

Designation	**Principal dimensions**			**Basic load ratings**		**Fatigue load limit**	**The safety factor**	**The maximal fatigue load**	**Bearing**
	d mm	D mm	H mm	C kN	C_0 kN	F_u kN	t_{-1}/τ_{P1}	$F_u^{(P1)}$ kN	
81110 TN	50	70	14	47.5	166	16.6	1.05	18.2	Cylindrical thrust roller
NUP 204 ECP	20	47	14	25.1	22	2.75	1.01	2.76	Cylindrical roller, $A_n = 4$
293/1600EF	1600	2280	408	36800	200000	11800	1.04	12900	Spherical roller thrust bearing

Summarizing, the following concluding remarks can be drawn:

1) The application of the multiaxial high-cycle criteria allows for the calculation of the equivalent fatigue stress including the non-proportional stress state which occurs in the rolling bearings,
2) The application of theoretical models based on the Hertz theory allows for the fast estimation of subsurface stress distribution, which is necessary when using the multiaxial high-cycle fatigue criteria,
3) The numerical results applied in the mathematical models and in the P_1 hypothesis give the similar values of the maximal fatigue load when comparing with the fatigue load limits F_u given by manufacturer.

REFERENCES

Belayev N. M.: Mag. Eng. Buildings and Applied Mech., St. Petersburg, 1924 (in Russian).

Bernasconi A., Filippini M., Foletti S., Vaudo D.: Multiaxial fatigue of a railway steel under non-proportional loading, International Journal of Fatigue, 2006, 28, p. 663–672.

Cooper D. H.: Tables of Hertzian contact-stress coefficients, University of Illinois, Report R-387, 1968.

Fessler H., Ollerton E.: Contact stresses in toroids under radial loads.Brit. J. appl. Phys., 1957, Vol. 8, pp. 387-393.

Hamiltion G. M., Goodman I. E.: The stress field created by a circular sliding contact, J. appl. Mech., 1966, Vol. 33, pp. 371-376.

Hamrock B. J., Anderson W. J.: Rolling-element bearings, Nasa Reference Publication 1105, 1983.

Krzeminski-Freda H.: Łożyska toczne, PWN, Warszawa 1989 (in Polish).

Hertz H.: Über die Berührung fester elastischer Körper, Journal für die reine und angewandte Mathematik, Vol. 92, 1881, pp. 156-171.

Hüber M. T.: Zur Theorie der Berührung fester elasticher Körper, Annal. Physik, Vol. 14, 1904, pp. 153-163.

Johnson K. L.: Contact mechanics, Cambridge university press, 2004.

Lundberg, G., and Palmgren, A.: Dynamic Capacity of Rolling Bearings, Acta Polytech. Scand., Mech. Eng. Ser., Vol. 1 (3), 1947, pp. 1–52.

Lundberg, G., and Palmgren, A.: Dynamic Capacity of Roller Bearings, Acta Polytech. Scand., Mech. Eng. Ser., Vol. 2 (4), 1952, pp. 96–127.

Ollerton E., Morey J. W.: Fatigue strength of rail steel in rolling contact, in Proc. Of the Symposium on Fatigue in rolling contact, IMechE, London, 1963, Vol. 2, pp. 11-22.

Papadopoulos I.V., Davoli P., Gorla C., Filippini M., Bernasconi A., A comparative study ofmultiaxial high-cycle fatigue criteria for metals. International Journal of Fatigue, 1997, Vol. 19(3), pp. 219-235.

Papuga J. A survey on evaluating the fatigue limit under multiaxial loading, International Journal of Fatigue, 2011, 33, p. 153–165.

Radzimovsky E. I.: Stress distribution and strength condition of two rolling cylinders pressed together, University of Illinois Bulettin, Vol. 50, No. 44. 1953, pp. 1-40.

Romanowicz P.: Fatigue analysis of selected machine elements working at rolling contact condition, PhD Thesis, Cracow University of Technology, Cracow 2010 (in Polish).

Romanowicz P.: Analiza wysokocyklowego wytężenia zmęczeniowego łożyska baryłkowego, Przegląd Mechaniczny, Vol. 11/12, 2012, pp.17-24 (in Polish).

Romanowicz P.: Application of selected multiaxial high-cycle fatigue criteria to rolling contact problems. Key Engineering Materials, Vol. 542, 2013, pp. 157-170.

Sackfield A., Hills D. A.: Some useful results in the classical Hertz contact problem, Journal of Strain Analysis, Vol. 18, No. 2, 1983, pp. 101- 105.

Sadeghi F., Jalalahmadi B., Slack T. S., Raje N., Arakere N. K.: A Review of Rolling Contact Fatigue, Journal of Tribology, Vol. 131, 2009, 041403.

Szybiński B., Romanowicz P., Zieliński A. P.: Numerical and experimental analysis of stress and strains in flat ends of high-pressure vessels, Key Engineering Materials, Vol. 490, 2012, pp. 226-236.

Thomas H. R., Hoersch V. A.: Stresses Due to the Pressure of one Elastic Solid uponAnother, Univ. of Ill. Eng. Exp. Sta. Bul., 1930, No. 212.

Timoshenko S., Goodier J. N.: Theory of Elasticity, McGraw-Hill Book Co., New York, 2nd edition, 1951.